Chapter 18.

Rate theory

S. Maillard[1], R. Skorek[1], P. Maugis[2], M. Dumont[2]
[1]CEA, DEN, DEC, Centre de Cadarache, France,
[2]Aix-Marseille Université, Université de Toulon, IM2NP UMR CNRS, France

Abstract

This chapter presents the basic principles of cluster dynamics as a particular case of mesoscopic rate theory models developed to investigate fuel behaviour under irradiation such as in UO_2. It is shown that as this method simulates the evolution of the concentration of every type of point or aggregated defect in a grain of material. It produces rich information that sheds light on the mechanisms involved in microstructure evolution and gas behaviour that are not accessible through conventional models but yet can provide for improvements in those models.

Cluster dynamics parameters are mainly the energetic values governing the basic evolution mechanisms of the material (diffusion, trapping and thermal resolution). In this sense, the model has a general applicability to very different operational situations (irradiation, ion-beam implantation, annealing) provided that they rely on the same basic mechanisms, without requiring additional data fitting, as is required for more empirical conventional models.

This technique, when applied to krypton implanted and annealed samples, yields a precise interpretation of the release curves and helps assess migration mechanisms and the krypton diffusion coefficient, for which data is very difficult to obtain due to the low solubility of the gas.

Cluster dynamics, a complementary method to mean-field models used in fuel performance codes for gas behaviour simulation

The behaviour of fission gases in fuel rods has been studied for decades and several performance codes [18,19,15,12]) have been developed to account for gas release and fuel swelling. These codes rely on "mean-field models" of a single grain (or a slab) considered as a "locally homogeneous" material for which diffusion-precipitation-resolution equations describe the evolution of the concentrations of fission gas atoms and bubbles

(xenon and krypton are the most abundant fission gases). The spatial variations of the concentrations across the grain can be taken into account to some extent, but very small scale variations, e.g., in close vicinity to bubbles or irradiation cascades, are smoothed, which justifies the terms "mean-field models" and "locally homogeneous". As an example, a set of equations (Equation 1a to Equation 1d) are shown below, similar to those solved by the Margaret code to model the behaviour of Xe in UO_2 [12]:

$$\partial_t(c+m) = \beta + D\Delta c \tag{1a}$$

$$\partial_t N = kc^2 - WN \tag{1b}$$

$$\partial_t m = 2kc^2 + 4\pi\frac{R}{\delta}RDNc - (W+w)m \tag{1c}$$

$$\partial_t m_v = \left(2kc^2 + 4\pi\frac{R}{\delta}RDNc - wm\right) + 4\pi RD_vN\delta c_v - Wm_v \tag{1d}$$

where c, N, m stand for the concentrations of dissolved Xe, nano-bubbles, and total precipitated Xe (in atoms or bubbles/cm^3), respectively, $m_v = \frac{4\pi R^3}{3\Omega}N$ is the total number of vacancies present in bubbles per unit volume (vacancies/cm^3, the same dimension as c, N and m), so that $m_v\Omega$ is the porosity of the material. β is the Xe source term, D the Xe diffusion coefficient, R the average radius of the bubbles. W and w are ballistic rates, the first one for bubble destruction and the second one for gas resolution (in s^{-1}). δc_v is a vacancy concentration differential explained below. δ is a distance characterising the gas capture.

Specifically:

- Equation 1a is the mass balance for Xe and describes total concentration changes through creation or diffusion.
- Equation 1b shows that the total number of bubbles (only nano-bubbles are addressed in this simplified example) changes through nucleation, which occurs when two Xe atoms encounter each other, or ballistic dissolution, when a fission spike reaches a bubble.
- Equation 1c accounts i) for the increase in the total concentration of precipitated Xe when a new bubble is created or when an existing bubble attracts an extra Xe atom; and ii) for its decrease when a bubble is destroyed or partially dissolved by a fission fragment.
- Equation 1d is similar to Equation 1c, taking into account the fact that the volume of the bubbles can grow through vacancy capture, proportional to $\delta c_v = c_v^{eq}(\infty) - c_v^{eq}(R)$, assuming that the bulk vacancy concentration follows the thermodynamic law ($c_v^{eq}(\infty) = \Omega^{-1}exp\left(-E_v^f/kT\right)$), and the vacancy concentration near the bubble depends on the bubble pressure P and surface energy γ ($c_v^{eq}(\infty) = \Omega^{-1}exp\left(-\left(E_v^f + \Omega(P-2\gamma/R)\right)/kT\right)$).

This kind of performance code relatively well reproduces the main operational features and post-irradiation observations resulting from the fuel evolution, in particular the gas concentration and release, swelling and porosity [4]. Many phenomena, however,

are included as empirical laws that do not depend upon a satisfactory and/or comprehensive understanding, thus reducing the reliability of the code when extrapolated beyond observations. For instance, at relatively high burn-up, a second type of bubbles of larger size appears at the centre of the fuel pellet [11]. In the model, this population does not appear as a result of nano-bubble evolution but is created according to an empirical relation. The analysis proposed in [4] shows that improvements in understanding should be achieved by taking into account the fact that the bubbles may exhibit distributed sizes and a gas content departing from the average. The bubble distribution could even be bimodal. Furthermore, a more realistic description of the bubble size and content evolution could be obtained by better accounting for the contribution of the isolated and aggregated self-defects generated in the material through the irradiation process. To our knowledge, no model including all these features has been applied to UO_2 in a PWR, especially in performance codes. Similar approaches are yet reported in [18] for high temperature of FBR fuel evolution. For instance, in the authors'own model, the bubbles are described by a discretised two-dimensional distribution function for radius and gas content, satisfying kinetic equations. The main mechanisms involved are bubble resolution and random or biased migration; the stoichiometry evolution is addressed as well and subsequent swelling and gas release are finally evaluated. In PWR fuels, [15] for instance, calculated the interstitial and vacancy bulk concentrations, as well as bubble average size and gas content, but not size distribution; [5] developed a cluster dynamics model that deals with the dislocation loop size distribution, but gas atoms and bubbles were not included in the model.

To improve the current operational models, a Cluster Dynamics (CD) model can be developed, aiming at calculating the time evolution of the concentration of clusters with various gas atom contents and sizes, as determined by elementary point defects (vacancies or self-interstitials).

Principle of cluster dynamics

Cluster dynamics is a chemical kinetics or rate theory method adapted to the simulation of the evolution of point defects, solutes and defect clusters (dislocation loops or bubbles) in materials at the grain scale [1]. In this method, the system investigated is seen as a gas of clusters of vacancies, interstitials and solute atoms; these clusters can show various sizes (including monomers). The properties of the system are spatially averaged and the positions of atoms or clusters are not considered, but spatial evolution of the cluster concentrations can be (but not described here). The evolution of the system is described by a set of differential equations on cluster concentrations and the model enables one to compute the evolution of the concentrations of all these clusters with time according to the various chemical reactions involved. Cluster Dynamics models have been extensively used in metallic systems, for example to study the behaviour of solid solutions in irradiated or non-irradiated metals [1].

Due to its low computer cost, cluster dynamics can handle long-term evolution that cannot be investigated through atomistic methods. Cluster dynamics enables the development of more general and precise models than standard operational rate theory models previously applied to nuclear fuels, which basically rely on the same physics, but make significant and poorly justified approximations on the cluster size distribution. In

comparison, the complete and unbiased description of the cluster size distribution can be computed by cluster dynamics as a natural consequence of input parameters such as formation and migration energies. Thus, such a model, as it addresses size and time scales relevant to industrial issues, appears as a natural framework for utilising atomic scale studies.

A drawback of the method is the loss of space correlations between the elements in the material microstructure which is the price to pay for the substantial decrease in computational cost compared to atomistic methods. Nevertheless, the improved description compared to earlier rate theory models comes with an increased complexity of numerical resolution. Finally, while cluster dynamics has been extensively applied to metallic systems, there are very few applications reported for ceramic fuels [5].

A cluster dynamics model for Kr behaviour in UO_2

The results presented below are from the European F-BRIDGE Project [14]. The goal was the first application of cluster dynamics modelling to the behaviour of fission gases, and especially Kr, in UO_2.

The CD model is devoted to calculating the time evolution of the concentration $C_{n,p}$ of aggregates of |n| elementary point defects (vacancies or self-interstitials) and p gas atoms (xenon or krypton); with the spatial dependence of these quantities not taken into account. By convention n is negative for vacancies, i.e., when clusters are voids or bubbles, and positive for self-interstitials, i.e., when clusters are dislocation loops. Loops incorporating gas atoms are not considered here. Because UO_2 is a diatomic material, several types of elementary defects should, in principle, be considered, as V_O, V_U, $V_U(V_O)_2$ for vacancies and O_i, U_i, $U_i(O_i)_2$ for interstitials. However the technique does not yet account for two different sub-lattices, so, in this study, we have assumed that vacancy and interstitial defects are $V_U(V_O)_2$ and $U_i(O_i)_2$ respectively, that is Schottky and anti-Schottky trios (or defects). Indeed, these defects are thought to be among the most favoured in the situations addressed here, namely close to stoichiometry [2]. Both elementary self-defects are supposed to be mobile and therefore likely to react with other point defects or clusters. The gas atoms are assumed to be mobile in two configurations, namely interstitial (i.e., (0,1) or Kr) or combined with a di-vacancy (i.e., (-2,1) or V_2Kr), as considered for various solutes in metals.

The evolution of each cluster concentration C(n,p) is controlled by a Master Equation [1,6]:

$$\partial_t C_{n,p} = \sum_{(m,q)mobile} J_{(n-m,p-q)+(m,q)\vec{\leftarrow}(n,p)} - \sum_{(m,q)mobile} J_{(n,p)+(m,q)\vec{\leftarrow}(n+m,p+q)} + G_{(n,p)} - K_{(n,p)} \quad (2)$$

where the first and second terms are the sums of the net cluster fluxes to and from the (n,p) cluster population, respectively. The third and fourth terms are the source and sink terms which account for the production of (n,p) defects inside the displacement cascades and their elimination to sinks (eg., free surfaces and grain boundaries) if they are mobile.

Each flux can be decomposed into absorption and emission rates:

$$J_{(n-m,p-q)+(m,q)\overrightarrow{\leftarrow}(n,p)} = B_{(n-m,p-q)+(m,q)\rightarrow(n,p)} C_{(n-m,p-q)} C_{(m,q)} - A_{(n,p)\rightarrow(n-m,p-q)+(m,q)} C_{(n,p)} \quad (3)$$

$B_{(n-m,p-q)+(m,q)\rightarrow(n,p)} C_{(n-m,p-q)} C_{(m,q)}$ is the absorption rate of the mobile cluster (m,q) by the cluster (n-m,p-q), yielding an (n,p) type cluster and $A_{(n,p)\rightarrow(n-m,p-q)+(m,q)} C_{(n,p)}$ is the emission rate of a mobile (m,q) cluster by an (n,p) type cluster, yielding an (n-m,p-q) type cluster. The flux $J_{(n-m,p-q)+(m,q)\overrightarrow{\leftarrow}(n,p)}$ can thus be related to the rates of a formal chemical reaction for $V_{-n}Xe_p$ dissociation (conventionally n<0 for vacancy containing clusters and n>0 for loops):

$$V_{-n}Xe_p \overrightarrow{\leftarrow} V_{-(n-m)}Xe_{p-q} + V_{-m}Xe_q.$$

$A_{(n,p)\rightarrow(n-m,p-q)+(m,q)}$ and $B_{(n-m,p-q)+(m,q)\rightarrow(n,p)}$ are absorption and emission coefficients, defined as:

$$B_{(n-m,p-q)+(m,q)\rightarrow(n,p)} = 4\pi\left(R_{(n-m,p-q)} + R_{(m,q)} + \delta R\right)\left(D_{(n-m,p-q)} + D_{(m,q)}\right)$$
$$A_{(n,p)\rightarrow(n-m,p-q)+(m,q)} = \left(B_{(n-m,p-q)+(m,q)\rightarrow(n,p)}/\Omega\right) exp\left(-\frac{F^b_{(n-m,p-q)+(m,q)\rightarrow(n,p)}}{kT}\right) \quad (4)$$

where, the R's are the radii of the various clusters, δR a capture radius allowing for small cluster recombination, the D's the diffusivities of the clusters and **Ω** the volume of the lattice unit cell. The right-hand side of Equation 4 is derived from the mass action law applied to the reaction. The binding free energy between the clusters, F^b, has been estimated on the basis of a conventional thermodynamic model, generalising Equation 9 [1]. A gas equation of state derived from a hard sphere model has been used in this model (Equation 29 [16]). The source term is evaluated with classical molecular dynamics [8].

Simulation of an annealing experiment using cluster dynamics

The cluster dynamics model as included in the code CRESCENDO [6] has been tested in Thermal Desorption Spectroscopy (TDS) experiments [9]. UO_2 samples have been irradiated at room temperature with 250 keV Kr ions at a very low fluence (0.5 s at a flux of 10^{12} Kr/cm^2/s). The samples have then been annealed at 1 250, 1 350, or 1 450^{0}C for about 800 minutes and the Kr release was monitored during the process. Because of the very low fluence, a rather small amount of irradiation vacancies are created; this partly prevents gas trapping and enhances the migration and release which benefits diffusivity measurements.

The krypton release curves from the annealing experiments at three temperatures are shown in Figure 1. Two release regimes can be distinguished: an initial burst (1st regime) is followed by a release roughly proportional to the annealing duration (2nd regime). Only the second follows the Fick's law.

If we focus on the second regime and neglect the initial bulk trapping of the mobile krypton, the fractional release, *F*, can be fitted by the approximate expression $F = Dt/L^2$ (*D* being the gas diffusivity, *L* the implantation depth).

A SRIM [17] simulation yields L = 70 nm, and from a subsequent numerical fitting, an average value of the krypton migration energy of ~ 4.5 eV has been obtained, according to the equation $D = \nu a^2 exp(-E_m/kT)$, ν being the Debye frequency (10^{13} Hz) and a the lattice parameter. Since DFT determination [7] of the Xe migration energy (1.6 eV) suggests that interstitial gas atoms are highly mobile, we assumed in this work, as developed below, that this rather low experimental diffusion coefficient corresponds to another mobile species, assumed to be V_2Kr. The released gas variation K of Equation 4 for a mobile krypton simply yields: $K = D\,C/L^2$ (C being the concentration of the corresponding krypton migrating species).

As stated above, the source term is evaluated on the basis of classical molecular dynamics simulations [8]. The cascade resulting from the implantation of a single ion (250 keV krypton ion or a fission product) is assumed to break down into 25 lower energy independent sub-cascades of ~ 10 keV each producing on average 20 Frenkel pairs: 3 cavities of 3 vacancies ((-3,0) or V_3), 3 loops of 3 self-interstitials ((3,0) or I_3), and 11 additional isolated interstitials ((1,0) or I) and vacancies ((-1,0) or V). Krypton is assumed to be inserted into an interstitial position during implantation ((0,1) or Kr).

A first CD simulation of the implantation yields the initial cluster concentrations. Two steps are calculated: the first one results from the 0.5 s implantation and simply reflects the production rates integrated over the implantation time; the second one is obtained after an annealing period at room temperature during which the very mobile self-interstitial defects (see Table 1) migrate to the free surface or other vacancies and annihilate.

Figure 1. Fraction of krypton released during the annealing experiment (solid lines: experiments, dotted lines: from fitting)

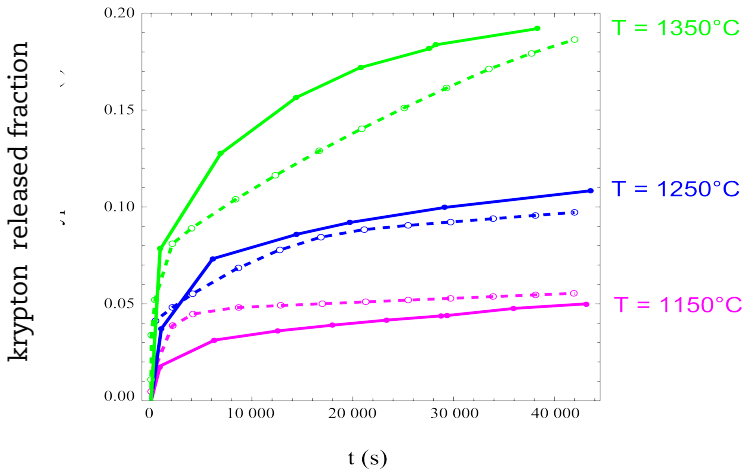

The formation and migration energies used in the model for the different elementary clusters are reported in Table 1. The formation energy of the self-interstitial is set at a very high value, practically preventing any thermal formation of Frenkel pairs while the other formation energies were taken from [3]. The migration energies are estimated by numerical fitting of the TDS experiments; initial estimates were based on atomistic

calculations of Xe migration energy [7] (assuming Kr and Xe have similar values) and on the Fickian analysis of the release curves for V_2Kr of Figure 1.

Table 1. Energetic and kinetic input parameters of the base defects (eV)

Defects	V (-1,0)	I (1,0)	Kr (0,1)	VKr (-1,1)	V_2Kr (-2,1)
Formation energies E_f^*	2.5	10	7	3.8	Thermodynamic model
Migration energies E_m^*	3	0.7	2.2	not mobile	4.5

Figure 2 shows the evolution of the different kinds of defects during annealing at 1 350°C. The figure and the corresponding reaction rates computed by CD reveal the following main features:

- The vacancies (green line) drive the system evolution, as they start to be mobile around 1 000°C: they aggregate to produce cavities (V_n) or bubbles (V_nKr_p) (summed for n>1 and represented by the thick green line); they also react with the loops and progressively "erode" them, finally yielding isolated interstitials according to reactions such as $nV + I_{n+1} \rightarrow I$. Eventually (t ~ 10^4 s), the vacancy concentration converges to the equilibrium value (doted green line).
- The self-interstitials I, produced through loop "erosion" by vacancies, represent an appreciable concentration (red line) as long as loops (thick red line) exist in the material (seen up to 1 000 s). This concentration has an important impact on the initial gas release.
- Indeed, gas atoms, initially implanted in interstitial position (Kr, cyan dotted line), are rapidly trapped, mostly by vacancies (in 10^{-4} s), yielding VKr (blue dotted line), which is not mobile. Further vacancy captures produce V_2Kr clusters (darker blue dotted line), which are again mobile. Both mobile species yield the cumulative krypton release of the doted black lines (Kr is thin, V_2Kr is thick).

The mechanisms of krypton release need some further analysis. Indeed, the very first burst of release is simultaneous with the trapping of interstitial krypton (Kr) by vacancies, and corresponds to its rapid migration to the grain free surface (first 10^{-4} s). An estimation of the time scale of Kr trapping by vacancies is $\tau = (4\pi RDC_V)^{-1} \approx 10^{-4}s$, which confirms that there should be no more Kr released after this period. A careful analysis of the higher reaction rates reveals an intense "kick-out" reaction involving an SIA the ejection of a substitutional Kr into an interstitial site by a SIA according to the reaction Kr: $VKr + I \underset{\leftarrow}{\overrightarrow{}} Kr$. This reaction accounts for Kr presence as long as free interstitial atoms exist, i.e., until complete annihilation of the loops by the mobile vacancies (t ~ 2 000 s). To summarise, krypton release can be explained by three successive mechanisms:

- t < 10^{-4} s: immediate release due to the migration of the initial interstitial krypton (Kr) while the rest remain trapped;
- 10^{-4} s < t < 2. × 10^3 s: release caused by interstitial krypton (Kr) produced by the kick-out reaction;

- 2. × 10^3 s < t: release caused by the substitutionally mobile (V_2Kr).

In conclusion, this first application of cluster dynamics to the interpretation of a TDS experiment yields interesting information, concerning mainly mechanisms, and, to some extent, energetic data.

- First, in such a modelling framework, two distinct krypton migration mechanisms (one interstitial and one substitutional) are necessary to explain the complex release curves, namely the initial burst.
- Second, migration energy can also be evaluated. For the krypton in substitutional position, the CD approach confirms the diffusivity evaluation obtained with a simple diffusion model applied to the late period of the experiments [9]. For the interstitial krypton, the fitting procedure yields a simultaneous and global estimation of the migration energies of all the remaining mobile species (I, V, Kr), which is less precise and should certainly be improved, for example through *ab initio* calculations or devoted experiments.
- Third, another important mechanism is evidenced as the "kick-out" reaction in which a self interstitial is replaced by a krypton atom in interstitial position. This mechanism basically relies on thermodynamic characteristics of the species involved in the reaction (i.e., the self-interstitial is much less soluble than the krypton), which motivates to determine more precisely the formation energy of the self-interstitial (i.e., anti-Schottky).

Figure 2. Concentration evolution of the main classes of clusters for the annealing experiment at 1 350°C

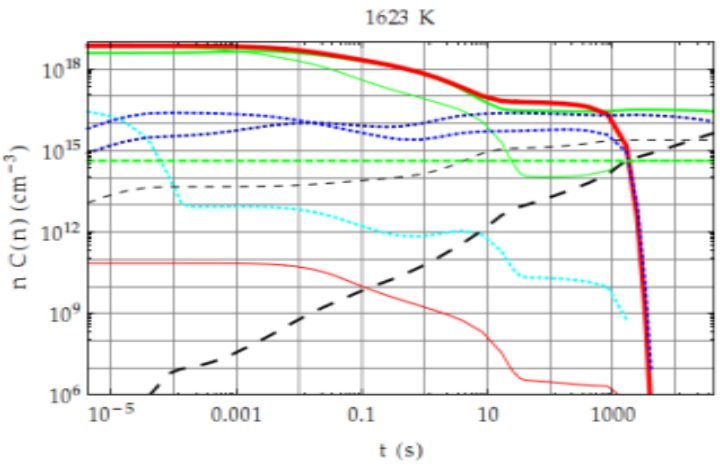

Conclusion and future challenges

Although cluster dynamics has long been applied to precipitation issues in metals, few examples exist concerning the behaviour of fission gas in PWR nuclear fuel. However, in this section, it has been demonstrated that the technique sheds light on aspects, and in particular mechanisms, which cannot be addressed with standard mesoscopic models used in fuel performance codes.

Cluster dynamics computes the evolution of the concentration of every type of point defect or cluster in a grain of material without any *a priori* choice concerning clusters or their reactions. As an interesting result of that, we have identified a potentially important "kick-out" mechanism that had not been anticipated prior to the calculations. Indeed, in-pile modelling of fission gas behaviour usually invokes ballistic gas resolution based on Nelson analysis [10] to account for the high dissolved concentration necessary to explain the gas release observed in irradiated UO_2. According to a recent evaluation of this resolution term [13] based on more precise techniques (coupled Monte Carlo/Molecular Dynamics), the gas resolution calculated by Nelson is 50 times too high; it can thus be inferred that this mechanism cannot alone explain the in-pile observed gas release. The kick-out mechanism, pointed out in this study, might be an additional possibility and should indeed be assessed in future work. In particular, CD should be validated on material undergoing irradiation.

Cluster dynamics, when applied to krypton implanted and annealed samples, yields a precise interpretation of the release curves and helps in assessing migration mechanisms. It also aids in the estimation of krypton diffusion coefficients, for which data are very difficult to obtain due to the low solubility of the gas.

Standard mesoscopic models are heavily phenomenological and rely on a rather limited set of effective parameters fitted from complex experiments, yet CD by contrast is based on a set of physical parameters (formation or migration energies of small clusters) describing the basic mechanisms (diffusion, capture, emission...) controlling the material's evolution; these parameters can be evaluated by atomistic methods or dedicated experiments. An advantage of the CD approach is that the same basic mechanisms describe various operational phenomena (ion implantation, neutron irradiation, annealing...), allow a unique set of parameters to be valid for all these situations. In the same way, the impact of minor changes in material characteristics (composition...) could ideally be assessed by CD based on separated effects experiments in which these physical parameters are determined. Ion-irradiation experiments could be used for such an initial assessment, prior to a more complex neutron irradiation. This would simplify the material's design process. Nevertheless, a temporary drawback of the approach is that the basic data necessary to assess the gas behavior in the material under irradiation remain difficult to obtain. Critical data may be missing or poorly known (migration energies of Kr, I, V, formation energy of I and I_2). More generally, a better knowledge of the real defects present in the material as a function of the stoichiometry is needed, so that the simplifying assumption of self-defects being equivalent to Schottky or anti-Schottky is better justified or improved. Indeed, in the near future, one can expect that basic data will be routinely available, from either atomistic calculations or dedicated experiments.

References

[1] Barbu, A., E Clouet (2007), *Solid State Phenomena*, 129, 51-58.

[2] Barthe, M.-F. et al. (2012), COSIRES, Santa Fe.

[3] Dorado, B. (2010), PhD Thesis, University of Aix Marseille II.

[4] Garcia, P. et al. (2011), NIMB, 227, 98.

[5] Jonnet, J. et al. (2008), NIMB, 266(12-13), 3008-3012.

[6] Jourdan, T. et al. (2014), *JNM*, 444(1-3), 298313.

[7] Liu, X.Y. et al. (2011), *Applied Physics Letter*, 98, 151902.

[8] Martin, G. et al. (2010), *Physics Letters* A, 374(30), 3038-3041.

[9] Michel, A. (2011), PhD Thesis University of Caen.

[10] Nelson, R.S. (1969), *Journal of Nuclear Materials*, 31(2), 153161.

[11] Noirot, J., Noirot, L. et al. (2004), *Proceedings of the 2004 International Meeting on LWR Fuel Performance,* Orlando, Florida.

[12] Noirot, L. (2011), *Nuclear Engineering and Design*, 241(6), 2099-2118.

[13] Schwen, D. et al. (2009), *Journal of Nuclear Materials*, 392(1), 3539.

[14] Skorek, R. (2013), PhD Thesis, University of Aix-Marseille.

[15] Veshchunov, M. S. et al. (2006), *Nuclear Engineering and Design*, 236(2), 179200.

[16] Volkov, A.E., A.I., Ryazanov (1999), *Journal of Nuclear Materials*, 273(2), 155-163.

[17] Ziegler, J.F. et al. (2012), *The Stopping and Range of Ions in Matter*.

[18] Griesmeyer, J.M. et al. (1979), "A dynamic intragranular fission gas behaviour model", *Nuclear Engineering and Design*, 55.

[19] Losonen, P. (2002), "Modelling intragranular fission gas release in irradiation of sintered LWR UO_2 fuel", *Journal of Nuclear Materials*, 304.